

MEASUREMENT OF THERMAL FLUXES AND ESTIMATION OF ELECTRODE TEMPERATURE IN A PULSED ELECTROMAGNETIC PLASMA ACCELERATOR

A. M. Rushailo

Zhurnal Prikladnoi Mekhaniki i Tekhnicheskoi Fiziki, No. 4, pp. 149-153, 1965

ABSTRACT: Some results of measurements of the total and radiative heat fluxes to the accelerating electrodes during a single capacitor discharge are presented for one model of an erosion-type coaxial plasma accelerator. On the basis of experimental data on the total heat transfer, the temperature at the surface of the accelerating electrodes is estimated.

Apparatus and measurement methods. The experimental device consisted of a IM5-150 capacitor bank with capacitance 1480 μf and the copper accelerating electrodes shown schematically in Fig. 1. The minimum inductance of the device was $\sim 9 \cdot 10^{-8}$ henry, and the working voltage range $U_0 = 2-5$ kV. The plasma was accelerated in a vacuum chamber at an initial pressure of $0,5 \cdot 10^{-4} - 1 \cdot 10^{-4}$ mm Hg.

The working medium was the products of erosion of the electrodes (copper) and, to a lesser degree, of the insulators (quartz, teflon).

The total plasma energy was measured by a calorimeter, the current by a Rogowski loop, and the voltage across the supply electrodes by a multi-range voltage divider.

As a result of the high magnetic induction in the pulsed accelerator, it was not possible to use the usual film sensor method for measuring the thermal fluxes. In this study the total thermal fluxes were measured using calorimetric thermal probes. As thermal probes we used cylindrical copper bodies up to 1 cm long mounted in the electrode wall. Teflon, plexiglas, and epoxy resin were used as electrical and thermal insulation.

The thermal probes work on the following principle. The thermal processes in the accelerator channel develop during the discharge time $t \sim 10^{-4}$ sec. In this interval the thermal wave penetrates the cold electrode wall or probe to a depth $h \sim (at)^{1/2}$, where a is the thermal diffusivity. For $t \sim 10^{-4}$ sec, $h \sim 0.01$ cm for copper. When the discharge ends, the temperature field of the probe is essentially nonuniform. The probe is completely heated after ~ 1 sec. Uniformity of the temperature field and cooling of the probe after complete heating are characterized by the Biot number ($B = al/\lambda$; a , λ , l are the heat transfer coefficient at the boundary, the thermal conductivity, and the characteristic length, respectively). For heat transfer with insulators $a < 0.01$; therefore, $B < 0.01$ for $l \leq 1$, and the temperature field of the probe can be assumed constant and only slightly dependent on time. Knowing the mass, heat capacity, and the area of the surface absorbing the heat flux, from the temperature measured for ~ 1 sec at any point of the probe the total heat flux to the probe can be determined.

The probe temperature was measured with a thermocouple and recorded by a EPP-09M potentiometer.

The radiation energy was determined by a radiometer based on the same calorimetric principle. In the radiometer, a thermal receiver with a blackened surface was isolated from the plasma by quartz glass. The quartz had a constant transparency throughout the experiment. The absorption region for quartz is below 2000 \AA .

Experimental results. Heat transfer to the outer and inner electrodes was measured along the generator and around the circumference of the inner electrode in sections A and B (Fig. 1). The working surface and mass of the outer and inner electrode probes were, respectively, 0.78 cm^2 , 0.53 g and 0.28 cm^2 , 1.3g. Experimental results for $U_0 = 3$ kV (initial energy $V_0 = 6.66 \cdot 10^3$ J) are plotted to a logarithmic scale in Fig 2. From the experimental points an average curve for the distribution of specific heat transfer over the length of the accelerator was constructed. The reduction in heat flux over length can be explained by the decrease in current density as the channel broadens. A small increase in heat transfer at the end of the accelerator is probably caused by a certain increase in current density due to a decrease in the magnetic field and the counter-emf at the end of the accelerator.

In the initial section of the accelerator, there is a considerable spread of the experimental points. This fact, also registered by every probe in section A, indicates considerable azimuthal nonuniformity of the discharge in the "throat." At a small distance from the "throat" (section B) the heat fluxes are relatively equivalent. The azimuthal nonuniformity of the discharge is probably caused by the arc-type current flow, which has already been noted in pulsed accelerators (for example, in [1]). Arc discharge in an accelerator may be one of the main causes of high energy losses.

The total heat transfer, equal to the integral of the mean-value curve over the electrode surface, is 600 J, or 9% of the initial energy, to the inner electrode and 1300 J, or 20%, to the outer electrode; 29 percent in all.

The losses determined by the probes are in good agreement with other measurements. The energy supplied to the accelerator, determined from current and voltage oscillograms, was 85% of the initial value. The efficiency of the device, or total plasma energy relative to initial energy, is 48% according to the calorimetric data. It follows that 37% of the initial energy is lost in the electrodes.

The thermal flux measured in the "throat" of the inner electrode through an opening 1 cm in diameter was compared to the radiation energy measured in the same place through a quartz screen. In each

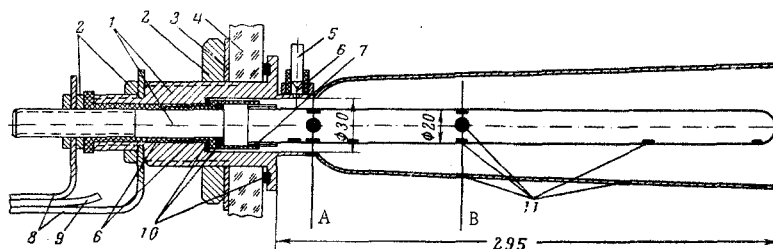


Fig. 1. Schematic of accelerating electrodes: 1) outer and inner electrodes; 2) nuts; 3) washers; 4) plexiglas flange; 5) firing electrode; 6) teflon insulating sleeves; 7) quartz insulator; 8) electrical leads; 9) vinyl chloride insulation; 10) vacuum rubber; 11) thermal probes.

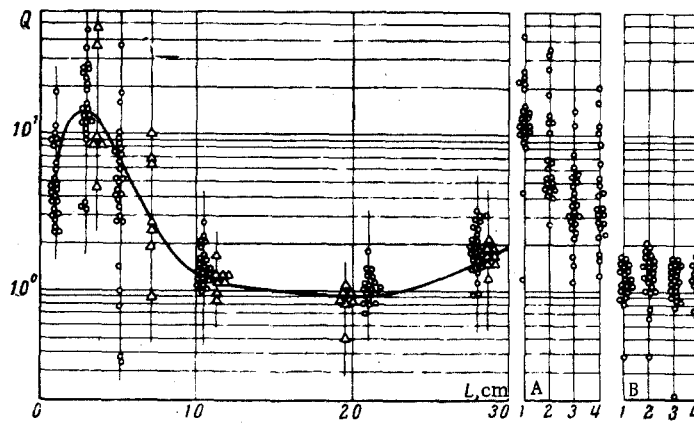


Fig. 2. Distribution of specific heat transfer Q ($J \cdot cm^{-2}$) to the inner (O) and outer (Δ) electrodes. The initial energy $V_0 = 6.66 \cdot 10^3 J$ ($U_0 = 3 kV$).

operating regime ($U_0 = 2-5 kV$) 25 experiments were performed. Average and maximum values of the radiation and specific heat transfer are given in Fig 3. The relative rms error in determining the average values was 0.15. Comparing the maximum and average values individually, we see that the radiation energy measured through the quartz screen is two orders less than the total heat transfer energy.

The amount of absorption by the quartz screen was estimated experimentally. A radiometer placed in a special housing and oriented in the direction of the outflowing stream was placed at the outlet section of the accelerating electrodes 8 cm from the axis. The main plasma flux did not touch the radiometer.

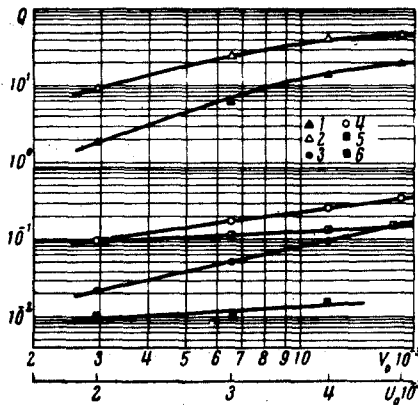


Fig. 3. Total and radiative heat transfer Q ($J \cdot cm^{-2}$) as a function of initial voltage U_0 , V (or initial energy V_0 , J); 1, 2) average and maximum heat transfer in "throat"; 3, 4) average and maximum radiation energy measured in the "throat" through a quartz screen; 5) radiation energy at the outlet measured with a screen; 6) measured without a screen.

It is clear from Fig 3 that the total (during discharge) energy flux measured by this radiometer without a quartz screen is ten times greater than the energy flux measured using a screen. Both screen absorption and the incidence of a small amount of plasma on the radiometer receiver may have caused this difference.

In any case, these experiments and the data obtained earlier show that absorption does not exceed 90%, while the radiation energy is not greater than 10% of the total heat transfer.

Estimating the temperature of the accelerating electrodes. To determine the temperature of the accelerating electrodes it is necessary to investigate the very difficult problem of the joint temperature

distribution in plasma and electrodes. However, for rough estimates the thermal problem can be considered separately at the electrodes alone.

Let us estimate the electrode surface temperature from experimental data on the total heat flux per unit surface during one discharge, assigning various laws of variation of the heat flux with time.

After discharge the depth of penetration of the thermal wave into the electrode is, as noted above, much less than the characteristic transverse dimensions. Therefore, the thermal problem for the electrodes may be replaced by the one-dimensional problem of non-stationary heat transfer in a semi-infinite body.

Let us write the heat transfer equation in dimensionless form

$$\frac{\partial \Psi}{\partial \xi} = \frac{\partial^2 \Psi}{\partial \eta^2} \quad (0 < \eta < \infty, 0 < \xi < \infty, \Psi = \frac{T - T_0}{\Delta T}), \quad (1)$$

$$\eta = \frac{x}{V a t_*}, \quad \xi = \frac{t}{t_*}, \quad \Delta T = \frac{Q \sqrt{a \pi}}{2 \lambda \sqrt{t_*}}.$$

Here T_0 , T are the initial and variable temperatures, x is the coordinate along the normal to the surface, t is time, t_* is the discharge half-period, ΔT is some characteristic quantity associated with the dimension of temperature, $a = \lambda / \rho c$ is the thermal diffusivity, and Q is the total heat flux during discharge per unit surface.

The initial boundary conditions for equation (1) are

$$\Psi(\eta, 0) = 0, \quad \frac{\partial \Psi(0, \xi)}{\partial \eta} = -\frac{2}{\sqrt{\pi}} \varphi(\xi) \quad (2)$$

$$\int_0^\infty \varphi d\xi = 1, \quad \varphi = \frac{q t_*}{Q}.$$

Here q is the specific heat flux at the boundary.

To explain the physical meaning of the quantity ΔT , let us consider equation (1) with the initial condition (2), the boundary condition $\Psi(0, \xi) = \delta = \text{const}$ ($0 < \xi \leq 1$), and $\varphi(\xi) = 0$ ($\xi > 1$). In this case, in the range $0 < \xi \leq 1$ we obtain the similar solution [2]

$$\Psi(\eta, \xi) = \delta [1 - \Phi(m)]$$

$$\left(m = \frac{\eta}{\sqrt{2\xi}}, \quad \Phi(m) = \frac{2}{\sqrt{2\pi}} \int_0^m \exp\left(-\frac{z^2}{2}\right) dz \right).$$

From (3), the second and third of relations (2), and the condition $\varphi = 0$ for $\xi > 1$, it follows that $\delta = 1$ and $\varphi = \frac{1}{2} \sqrt{\xi}$ for $0 < \xi \leq 1$.

Thus, the characteristic quantity ΔT is the difference between the maximum surface temperature and the initial temperature of the

body for the problem with the self-similar condition $\Psi(0, \xi) = \text{const}$ for $0 < \xi \leq 1$ and $\varphi(\xi) = 0$ for $\xi > 1$.

In the first approximation, it follows from the current and voltage oscillograms that all thermal processes in the channel take place during the first current half-period $\tau_c = 4 \times 10^{-5}$ sec. For copper, $\lambda = 3.94$ J/cm·deg·sec, while $A = 1.13$ cm²/sec; consequently, $\Delta T = 38.3Q$. The characteristic surface heating may prove higher than the melting point of copper (1083°C) if $Q > 30$ J/cm². In fact, in experiments under these conditions (see Fig. 3) traces of melting were detected on the surfaces of the probes and electrodes.

The solution of equation (1) with condition (2) in general form is [2]

$$\Psi(\eta, \xi) = \frac{2\sqrt{2}}{\pi} \int_m^\infty \eta \left(\xi - \frac{\eta^2}{2z^2} \right) \frac{\exp(-1/2z^2)}{z^3} dz \quad \begin{matrix} 0 < \eta < \infty, \\ 0 < \xi < \infty, \end{matrix}$$

$$m = \frac{\eta}{\sqrt{2\xi}} \quad (4)$$

We assume that the function φ permits a Taylor expansion in a small neighborhood of the point ξ taken from some interval of values. In this interval

$$\Psi(\eta, \xi) = \frac{4}{\pi} \sum_{n=0}^\infty (-1)^n \frac{1}{n!} \left(\frac{\eta}{\sqrt{2}} \right)^{2n+1} \varphi^{(n)}(\xi) \int_m^\infty \frac{\exp(-1/2z^2)}{z^{2(n+1)}} dz \quad (5)$$

In order to remove the indeterminacy at $\eta = 0$, we replace the integral in expression (5) by the recurrence relation from equation (3.461) of [3]

$$\Psi(\eta, \xi) = \frac{4}{\pi} \sum_{n=0}^\infty (-1)^n \left(\frac{\eta}{\sqrt{2}} \right)^{2n+1} \varphi^{(n)}(\xi) \times$$

$$\times \left\{ \frac{(-1)^{n+1} \sqrt{\pi}}{\sqrt{2}(2n+1)!} \left[1 - \Phi\left(\frac{\eta}{\sqrt{2\xi}}\right) \right] + \right.$$

$$\left. + \left(\frac{\sqrt{2\xi}}{\eta} \right)^{2n+1} \left(\exp \frac{-\eta^2}{4\xi} \right) \times \right.$$

$$\left. \times \sum_{k=0}^n \frac{(-1)^k}{(2n+1)(2n-1)\dots(2n-2k+1)} \left(\frac{\eta}{2\sqrt{\xi}} \right)^{2k} \right\}$$

Passing to the limit as $\eta \rightarrow 0$, we find the surface temperature

$$\Psi(0, \xi) = \frac{4}{\pi} \sum_{n=0}^\infty (-1)^n \frac{(\sqrt{\xi})^{2n+1} \varphi^{(n)}(\xi)}{n!(2n+1)} \quad (6)$$

The heat release in the accelerator is proportional to the square of the current, and in the first approximation the current depends upon time as $I \sim \exp(kt)\sin(\pi t/\tau_c)$. Therefore it is of interest to determine, together with the similar solution, the surface temperature for the following laws of variation of the heat flux:

$$\varphi_3 = 1, \quad \varphi_3 = 1/2\pi \sin \pi \xi, \quad \varphi_4 = 2 \sin^2 \pi \xi \quad (0 < \xi \leq 1),$$

$$\varphi_3 = \varphi_3 = \varphi_4 = 0 \quad (\xi > 1), \quad (7)$$

$$\varphi_5 = 4\pi \varepsilon (1 + \varepsilon^2) e^{-2\pi \varepsilon \xi} \sin^2 \pi \xi \quad (0 < \xi < \infty).$$

Here $\varepsilon = kt_c/\pi$, and all the functions $\varphi(\xi)$ are chosen so as to satisfy the third relation of (2).

1. The surface temperature for $\varphi_2 = 1$ in the range $0 < \xi \leq 1$ is easily determined from (6) and coincides with the first part of the complete solution [2]

$$\Psi_1(0, \xi) = 4\pi^{-1} \sqrt{\xi} \quad (0 < \xi \leq 1),$$

$$\Psi_2(0, \xi) = 4\pi^{-1} (\sqrt{\xi} - \sqrt{\xi-1}) \quad (\xi > 1). \quad (8)$$

2. For the case $\varphi_3 = \pi \sin \pi \xi / 2$ ($0 < \xi \leq 1$), we separate the odd and even derivatives of $\varphi_3(\xi)$ and represent (6) in the form of the sum

of two series, each of which is one of the Fresnel integrals [3]

$$\Psi_3(0, \xi) = \sqrt{2} [C(\sqrt{\pi\xi}) \sin \pi \xi - S(\sqrt{\pi\xi}) \cos \pi \xi] \quad (0 < \xi \leq 1),$$

$$S(x) = \frac{2}{\sqrt{2\pi}} \int_0^x \sin t^2 dt = \frac{2}{\sqrt{2\pi}} \sum_{n=0}^\infty \frac{(-1)^n x^{4n+3}}{(2n+1)!(4n+3)}, \quad (9)$$

$$C(x) = \frac{2}{\sqrt{2\pi}} \int_0^x \cos t^2 dt = \frac{2}{\sqrt{2\pi}} \sum_{n=0}^\infty \frac{(-1)^n x^{4n+1}}{(2n)!(4n+1)}$$

3. Note that $\varphi_4 = 1 - \cos 2\pi\xi$. Separating, as before, the odd and even derivatives of $\varphi_4(\xi)$, we find

$$\Psi_4(0, \xi) = 4\pi^{-1} \{ \sqrt{\xi} - 1/2 [S(\sqrt{2\pi\xi}) \sin 2\pi\xi + C(\sqrt{2\pi\xi}) \cos 2\pi\xi] \}. \quad (10)$$

4. The function φ_5 can be represented in the following form:

$$\varphi_5 = 2\pi \varepsilon (1 + \varepsilon^2) [e^{-2\pi \varepsilon \xi} - Re e^{2\pi \varepsilon (i-\varepsilon)\xi}]$$

$$(i = \sqrt{-1}, 0 < \xi < \infty). \quad (11)$$

Substituting the derivatives of both terms of (11) in (6), after elementary, but awkward operations we obtain

$$\Psi_5(0, \xi) = 8\varepsilon (1 + \varepsilon^2) \sqrt{\xi} \left\{ \frac{W(\sqrt{2\pi\varepsilon\xi})}{\sqrt{2\pi\varepsilon\xi}} - Re \frac{W[\sqrt{2\pi\xi}(\varepsilon-i)]}{\sqrt{2\pi\xi}(\varepsilon-i)} \right\}. \quad (12)$$

Here $W(z)$ is the probability function in the complex domain

$$W(z) = e^{-z^2} \int_0^z e^{\alpha^2} d\alpha$$

Values of (3), (8), (9), (10) and (12), obtained using the tables in [4-6], are given in Fig. 4. In the calculations, the value $\varepsilon = 0.364$ for Ψ_5 was taken from the current oscillogram. It is clear from the graph that the difference in the maximum values of the surface temperature is small and does not exceed one half the characteristic estimated value of ΔT for the heat fluxes considered.

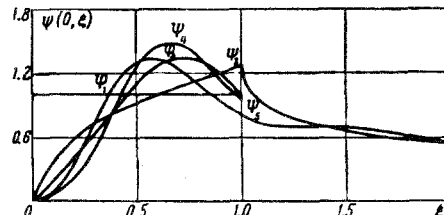


Fig. 4. Surface temperature as a function of time for different heat fluxes.

The author thanks G. M. Bam-Zelikovich and A. B. Vatazhin for their interest in his work.

REFERENCES

1. T. J. Gooding, B. R. Hayworth, and R. H. Lovberg, "Instabilities in a coaxial plasma gun," Amer. Inst. Aeronaut. and Astronaut. Journal, vol. 1, no. 6, p. 1289-1292, 1963.
2. H. S. Carslaw and J. C. Jaeger, Conduction of Heat in Solids [Russian translation], Izd-vo "Nauka," 1964.
3. I. S. Gradshteyn and I. M. Ryzhik, Tables of Integrals, Sums, Series, and Products [in Russian], Fizmatgiz, 1962.
4. Library of Mathematical Tables, no. 3, Tables of Probability Functions [in Russian], Computing Center AS USSR, vol. 2, 1959.
5. Tables of Fresnel Integrals [in Russian], ed. V. A. Ditkin, Izd-vo AN SSSR, 1963.
6. K. A. Karpov, Tables of the Function $W(z) = e^{-z^2} \int_0^z e^{\alpha^2} d\alpha$ in the Complex Domain [in Russian], Izd-vo AN SSSR, 1954.